International Journal of Mechanical, Industrial and Aerospace Sciences
ISSN: 2517-9950
Vol:6, No:9, 2012

Simulation of Natural Convection in Concentric Annuli between an Outer Inclined Square Enclosure and an Inner Horizontal Cylinder

Sattar Al-Jabair, Laith J. Habeeb

Abstract**—**In this work, the natural convection in a concentric annulus between a cold outer inclined square enclosure and heated inner circular cylinder is simulated for two-dimensional steady state. The Boussinesq approximation was applied to model the buoyancy-driven effect and the governing equations were solved using the time marching approach staggered by body fitted coordinates. The coordinate transformation from the physical domain to the computational domain is set up by an analytical expression. Numerical results for Rayleigh numbers 10^3 , 10^4 , 10^5 and 10^6, aspect ratios 1.5 , 3.0 and 4.5 for seven different inclination angles for the outer square enclosure 0^o , -30^o , -45^o , -60^o , -90^o , -135^o , -180^o are presented as well. The computed flow and temperature fields were demonstrated in the form of streamlines, isotherms and Nusselt numbers variation. It is found that both the aspect ratio and the Rayleigh number are critical to the patterns of flow and thermal fields. At all Rayleigh numbers angle of inclination has nominal effect on heat transfer.

Keywords**—**natural convection, concentric annulus, square inclined enclosure

I. Introduction

NATURAL convective heat transfer in annuli has attractedmany attentions in recent years due to its wide industrial and environmental applications such as in heat exchangers, nuclear and chemical reactors design, cooling of electronic equipment, aircraft cabin insulation, stratified atmosphere boundary layers and thermal storage system.A large and diverse number of literatures on both experimental and numerical investigations were published in the past few decades. Comparatively, little work has been done on natural convective heat transfer in more complex annuli such as the problem considered in this study. In engineering applications, the geometries that arise are more complicated than a simple enclosure filled with a convective fluid. The geometric configuration of interest is coupled with the presence of bodies embedded within the inclined enclosure.

Many investigations have dealt with numerical calculations for natural convection induced by a temperature difference between a cold outer square cylinder and a hot inner circular cylinder for different Rayleigh numbers and aspect ratios or circular cylinder's positions.

C. Shu and Y. D. Zhu[1] simulate the natural convection in a concentric annulus using the deferential quadrature (DQ) method. Numerical results for Rayleigh numbers (*Ra*) range from 10^4 to 10^6 and aspect ratios between 1.67 and 5.0 are presented, which were in a good agreement with available data in the literature.

Sattar Al-Jabair is Assist Prof. in Mech. Eng. Dept. University of Technology, Baghdad, Iraq. (Email:drsattar@uotechnology.edu.iq)
Laith J. Habeebis Lecturer in Mech. Eng. Dept. University of Technology, Baghdad, Iraq.(Email:dr.laith_jaafer@uotechnology.edu.iq)

B.S. Kim *et. al*.[2] obtained a two-dimensional solution for unsteady natural convection using the immersed boundary method (IBM) to model an inner circular cylinder based on the finite volume method for different Rayleigh numbers varying over the range of 10^3–10^6. Hyun SikYoon*et. al.* [3] investigated the effect of the inner cylinder location on the heat transfer and fluid flow for Rayleigh number = 10^7. Within two critical positions, the thermal and flow fields are steady state. In the unsteady region, the natural convection shows a single frequency and multiple frequency periodic patterns alternately according to the two critical positions.

The changes in heat transfer quantities have also been presented. Hakan F.Oztop*et. al.*[4] studied mixed convection heat transfer characteristics for a lid-driven air flow within a square enclosure having a circular body. The computation is carried out for wide ranges of Richardson numbers, diameter of inner cylinder and center and location of the inner cylinder. It was found that the most effective parameter on flow field and temperature distribution is the orientation of the moving lid.

The circular body can be a control parameter for heat and fluid flow. J.M. Leeet. al.[5] investigated both effects of the inner cylinder location in an enclosure and the buoyancy-induced convection on heat transfer and fluid flow. The existence of local peaks of the Nusselt number along the surfaces of the cylinder and the enclosure is determined by the gap and the thermal plume governed by the conduction and the convection, respectively. Salam Hadi Hussain and Ahmed Kadhim Hussein [6] studied the effects of vertical cylinder locations and Rayleigh numbers on fluid flow and heat transfer performance for circular cylinder immersed in square enclosure. It is found that the numerical solutions yield a two cellular flow field between the inner cylinder and the enclosure.

Most of the numerical studies were carried out by use of the finite difference, finite volume, and finite element methods. Moreover, efforts have been performed to study natural convection in different shape annuli either with circular cross-sections or with non-circular cross-sections, which typically include rectangle enclosure with square/circular inner cylinder, cylindrical enclosure with an inner coaxial triangular cylinder and inner sphere with outer vertical cylinder.

TalalKassem [7] deals with numerical prediction of natural convection heat transfer in the annular space between the circular receiver tube and the glass envelope in the so parabolic–cylindrical solar collector, for the case of an isothermal outer cylinder with a sinusoidal local heat flux distribution on the inner cylinder. The two-dimensional structures of the fluid flow and temperature distributions as well as local and average Nusselt numbers are obtained.

C. Shuet. al. [8] studied the effect of eccentricity and angular position on the flow and thermal fields for circular inner cylinder. Arnab Kumar De and AmareshDalal [9] studied the effects of the enclosure geometry using three different aspect ratios placing the square cylinder at different heights from the bottom. It is found that the uniform wall temperature heating is quantitatively different from the uniform wall heat flux heating. Flow pattern and thermal stratification are modified, if aspect ratio is varied. Overall heat transfer also changes for different aspect ratio. WenRuey Chen [10] investigated the effects of eccentricity and geometric configuration to determine heat transfer by natural convection between the sphere and vertical cylinder. Results of the parametric study conducted further reveal that the heat and flow fields are primarily dependent on the Rayleigh number, eccentricity and geometric configuration, for a Prandtl number of 0.7, with the Rayleigh number ranging from 10^3 to 10^6, the three eccentricities and two geometric configurations. Xuet. al. [11] conducted numerical simulation to investigate the steady laminar natural convective heat transfer for air within the horizontal annulus between a heated triangular cylinder and its circular cylindrical enclosure. Four different Rayleigh numbers and four different radius ratios were considered, and four different inclination angles for the inner triangular cylinder were investigated as well. Zi-Tao Yu et. al. [12] performed numerical study of laminar convection heat transfer from a horizontal triangular cylinder to its concentric cylindrical enclosure to investigate the Prandtl number effect on flow and heat transfer characteristics. The entire spectrum of Prandtl number investigated can be divided into three sections based on the variations of average heat transfer coefficients.

The study of natural convection of an inclined cavity and the influence of the angle of inclination is studied with the view to know the effect of angle, on the heat transfer characteristics. Manab Kumar Das and K. Saran Kumar Reddy [13] concerned with the computation of natural convection flow in a square enclosure with a centered internal conducting square block both of which are given an inclination angle. Solution has been performed in the computational domain as a whole with proper treatment at the solid/fluid interface. YasinVarolet. al. [14] studied numerically the phenomena of natural convection in an inclined square enclosure heated via corner heater. One wall of the enclosure is isothermal but its temperature is colder than that of heaters while the remaining walls are adiabatic. It is observed that heat transfer is maximum or minimum depending on the inclination angle and depending on the length of the corner heaters. H.F. Nouanegueet. al. [15] investigated conjugate heat transfer by natural convection, conduction and radiation in an inclined square enclosure bounded by a solid wall with its outer boundary at constant temperature while the opposing active wall is with a constant heat flux. F.A. Muniret. al. [16] reported the fluid flow behavior and the characteristic of heat transfer from a differentially heated enclosure walls and tilted at various inclination angles.

It found that the vortex formation, size and flow characteristics were significantly affected by the magnitude of inclination angles.

II. Problem Description and Mathematical Model

A schematic of the system considered in the present study is shown in Fig. 1. The system consists of a square enclosure with sides of length L, within which a circular cylinder located at the center of the enclosure with aspect ratios ($Ar = L/r_i$) equals to 1.5 , 3.0 and 4.5 and seven different inclination angles (ϕ) for the outer square enclosure 0^o , -30^o , -45^o , -60^o , -90^o , -135^o and -180^o . The walls of the square enclosure were kept at a constant low temperature, whereas the cylinder was kept at a constant high temperature. In this study, it assumed that the radiation effects are negligible. The fluid properties are also assumed to be constant, except for the density in the buoyancy term, which follows the Boussinesq approximation. The gravitational acceleration acts in the negative *y*-direction. As the circular cylinder and the square enclosure are long enough, so the flow is consider being steady, laminar and two dimensions. The enclosure filled with air and Prandlt number (Pr) = 0.71.

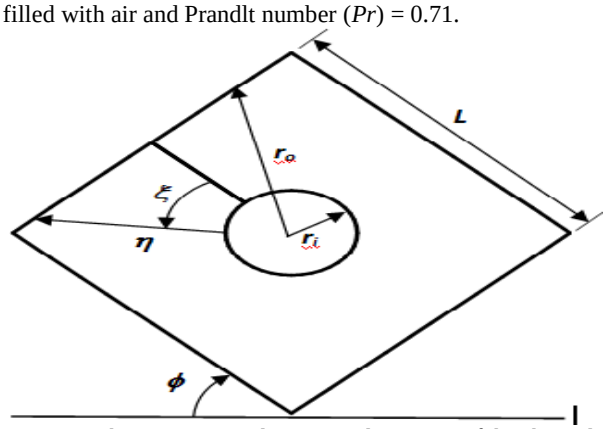

Fig. 1 A schematic view and geometry description of the physical domain

The dimensionless governing equation for the problem is written in the stream – vorticity formulation as in reference eight:

$$\frac{\partial^2\psi}{\partial x^2}+\frac{\partial^2\psi}{\partial y^2}=\omega \tag{1}$$

$$u\frac{\partial\psi}{\partial x}+v\frac{\partial\psi}{\partial y}=Pr\left(\frac{\partial^2\omega}{\partial x^2}+\frac{\partial^2\omega}{\partial y^2}\right)-Pr\,Ra\left(\frac{\partial T}{\partial x}sin\phi-\frac{\partial T}{\partial y}cos\phi\right) \tag{2}$$

$$u\frac{\partial T}{\partial x}+v\frac{\partial T}{\partial y}=\frac{\partial^2 T}{\partial x^2}+\frac{\partial^2 T}{\partial y^2} \tag{3}$$

Whereϕ in (deg.), hence, introducing the following non-dimensional variables:

$$Pr=\mu C_P/k \quad , \quad Ra=C_P\,\rho_0\,g\,\beta\,L^3\Delta T^*/(k\,v)$$

$$T=\frac{T^*-T_o^*}{\Delta T^*} \quad , \quad \omega=\frac{\omega^* L^*}{v_\infty^*} \quad , \quad \psi=\frac{\psi^*}{L^* v_\infty^*} \quad , \quad v_\infty^*=\frac{k}{L}$$

Where Cp in (J/kg K), k in (m^2/sec), ρ_0 in(kg/m^3), β in (1/K), ν in (m^2/sec) and the velocity components u and v can be computed from the stream function ψ as:

$$u = \frac{\partial \psi}{\partial y} \quad , \quad v = -\frac{\partial \psi}{\partial x} \tag{4}$$

Using the expressions in Equation (4), Equation (1) can be written as:

$$\omega = \frac{\partial u}{\partial y} - \frac{\partial v}{\partial x} \tag{5}$$

Then, using the following transformation from the physical space to the computational space:

$$\left.\begin{aligned} \xi &= \xi(x, y) \\ \eta &= \eta(x, y) \end{aligned}\right\} \tag{6}$$

With this transformation, the governing Equations (1) to (3) can be transformed to the following forms in the computational space:

$$A\frac{\partial^2 \psi}{\partial \xi^2} + 2B\frac{\partial^2 \psi}{\partial \eta \partial \xi} + C\frac{\partial^2 \psi}{\partial \eta^2} + G\frac{\partial \psi}{\partial \eta} + H\frac{\partial \psi}{\partial \xi} = J\omega \tag{7}$$

$$U\frac{\partial \omega}{\partial \xi} + V\frac{\partial \omega}{\partial \eta} = Pr\,(AU\frac{\partial^2 \omega}{\partial \xi^2} + 2BU\frac{\partial^2 \omega}{\partial \xi \partial \eta} + CU\frac{\partial^2 \omega}{\partial \eta^2} + GU\frac{\partial \omega}{\partial \eta} + HU\frac{\partial \omega}{\partial \xi}) - Pr\,Ra\left(y_\eta \frac{\partial T}{\partial \xi}\sin\phi - y_\xi \frac{\partial T}{\partial \eta}\cos\phi\right) \tag{8}$$

$$U\frac{\partial T}{\partial \xi} + V\frac{\partial T}{\partial \eta} = Pr(A\frac{\partial^2 T}{\partial \xi^2} + 2B\frac{\partial^2 T}{\partial \xi \partial \eta} + C\frac{\partial^2 T}{\partial \eta^2} + G\frac{\partial T}{\partial \eta} + H\frac{\partial T}{\partial \xi}) \tag{9}$$

Where:

$$U = \frac{\partial \psi}{\partial \eta} = u\,y_\eta - v\,x_\eta \quad , \quad V = -\frac{\partial \psi}{\partial \xi} = v\,x_\xi - u\,y_\xi \ , \ A = \alpha/J \ ,$$

$$B = -\sigma/J \ , \ C = \gamma/J \ , \ G = \frac{\partial B}{\partial \xi} + \frac{\partial C}{\partial \eta}, \ H = \frac{\partial A}{\partial \xi} + \frac{\partial B}{\partial \eta} \quad ,$$

$$\alpha = x_\eta^2 + y_\eta^2 \ , \ \sigma = x_\xi x_\eta + y_\xi y_\eta \ , \ \gamma = x_\xi^2 + y_\xi^2 \ , \ J = x_\xi x_\eta - y_\xi y_\eta$$

III. Grid Generation

In this study, an analytical expression could derive for the coordinate transformation from the physical domain to the computational domain; all-geometrical parameters could compute exactly. The super elliptic function could be written as:

$$\left(\frac{x}{a}\right)^{2n} + \left(\frac{y}{b}\right)^{2n} = 1 \tag{10}$$

Where $a$and$b$ are the square enclosure lengths in the x and y direction respectively, n is a positive integer. So for this study it could be expressed as: n = 100; a = b, the geometry becomes a square with minimum error.

The coordinate's transformation for the present problem can be exactly setup, which is written as:

$$x = -\sin\xi \cdot [r_i + (r_o - r_i)\eta] \tag{11a}$$

$$y = \cos\xi \cdot [r_i + (r_o - r_i)\eta] \tag{11b}$$

Where r_i is the radius of the inner circular cylinder, which is a constant, and r_o is the equivalent radius of the outer square enclosure and it is computed as in reference one:

$$r_o = \frac{b}{\left(\cos(\xi)^{2n} + \sin(\xi)^{2n}\right)^{1/2n}} \tag{12}$$

The transformed computational domain to (ξ,η) plane is $0 \le \eta \le 1$ and $0 \le \xi \le 2\pi$. A typical generated grid is shown in Fig. 2, for 41×41 nodes.

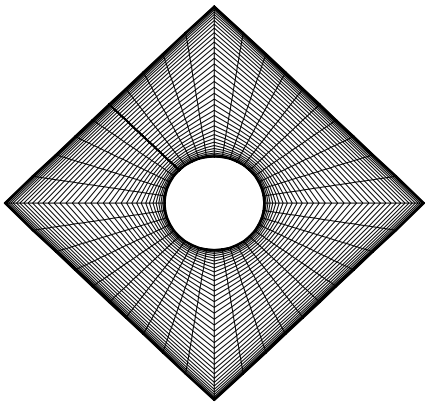

Fig. 2 A typical grid generation (41×41 grids) for ϕ = -45°, r_i = 0.5, $L = 3r_i$, n = 100

The imposed boundary conditions are no slip and isothermal on both inner circular cylinder and outer square enclosure surfaces. Therefore, the boundary conditions could be express as:

$$U\big|_{\eta=0,1} = 0 \quad , \quad V\big|_{\eta=0,1} = 0 \tag{13a}$$

$$\psi\big|_{\eta=0} = 0 \quad , \quad \psi\big|_{\eta=1} = 0 \tag{13b}$$

$$T\big|_{\eta=0} = 1 \quad , \quad T\big|_{\eta=1} = 0 \tag{13c}$$

$$\omega\big|_{\eta=0,1} = \frac{C}{J}\frac{\partial^2 \psi}{\partial \eta^2}\bigg|_{\eta=0,1} = \frac{C}{J}\frac{\partial U}{\partial \eta}\bigg|_{\eta=0,1} \tag{13d}$$

IV. Numerical Method

In this work the finite difference equation were derived by using central difference approximation for the partial derivatives except the convective terms for which upwind difference formula was employed. Derivative at the boundary were approximated by three point forward or backward difference. The explicit method was chosen for the solution of flow and energy fields, while relaxation method was chosen for stream function calculation. A time increment 10^{-5} - 10^{-9} has been used for Ra=10^3 - 10^6.

The average Nusselt numbers for the inner and outer boundaries are respectively determined by (Ref.[1]):

$$\overline{Nu}_i = \frac{\bar{h}_i S_i}{k} \quad \text{and} \quad \overline{Nu}_o = \frac{\bar{h}_o S_o}{k} \tag{14}$$

Where

$$\bar{h} = \frac{1}{2\pi}\int_0^{2\pi} h.d\xi \quad \text{and} \quad h = -k\frac{\partial T}{\partial \eta}.\frac{\sqrt{\gamma}}{J} \tag{15}$$

V. Grid Independency Study

Several grids have been tested for the case of $Ra = 10^3$, $\phi = 0$, $r_i = 0.5$, $L = 1.5r_i$. Table I shows the total average Nusselt number for five grids used.

TABLE I
Nu_{ave} Results For Several Grids, $Ra = 10^3$, $\phi = 0$, $R_i = 0.5$, $L = 1.5R_i$.

Grid size	$Nu_{ave} = \frac{\overline{Nu}_i + \overline{Nu}_o}{2}$	$\lvert\psi_{max}\rvert$
21×21	3.384678	0.128155
30×30	3.345281	0.13814
41×41	3.335432	0.123844
50×50	3.329070	0.129731
61×61	3.322617	0.13704

It can be see that, a little difference between the sets of grid results and the grid of 41×41 is used in all subsequent calculation of this study to decrease the time cost of the solution convergence, without effecting in the solution accuracy.

VI. Validation Test

The calculations of average Nusselt numbers for the test case are compared with the benchmarks values of C. Shu and Y. D. Zhu[1] , B.S. Kim et. al.[2] for different values of Rayleigh number as given in table II. The differences are due to the computational domain was taken as half of the physical domain in Ref.[1], the Nusselt numbers were taken along the hot wall only in Ref.[2] and small grid size was taken in present work.

TABLE II
Comparison of the present average Nusselt number with references one and two

Ra	Ref.[1]	Ref.[2]	Present study
10^4	3.24	3.414	3.676834
10^5	4.86	5.1385	4.801162

In addition, the validation test data of the streamline and isothermal contours compared with the results of [2], and, [5] for Rayleigh number = 10^3, (L/D) = 0.4) and with the results of Ref.[1] for Rayleigh number = 10^4, (L/D = 0.2) are shown in Fig. 3.

(a) [2]

(b) [5]

(c)

(d)

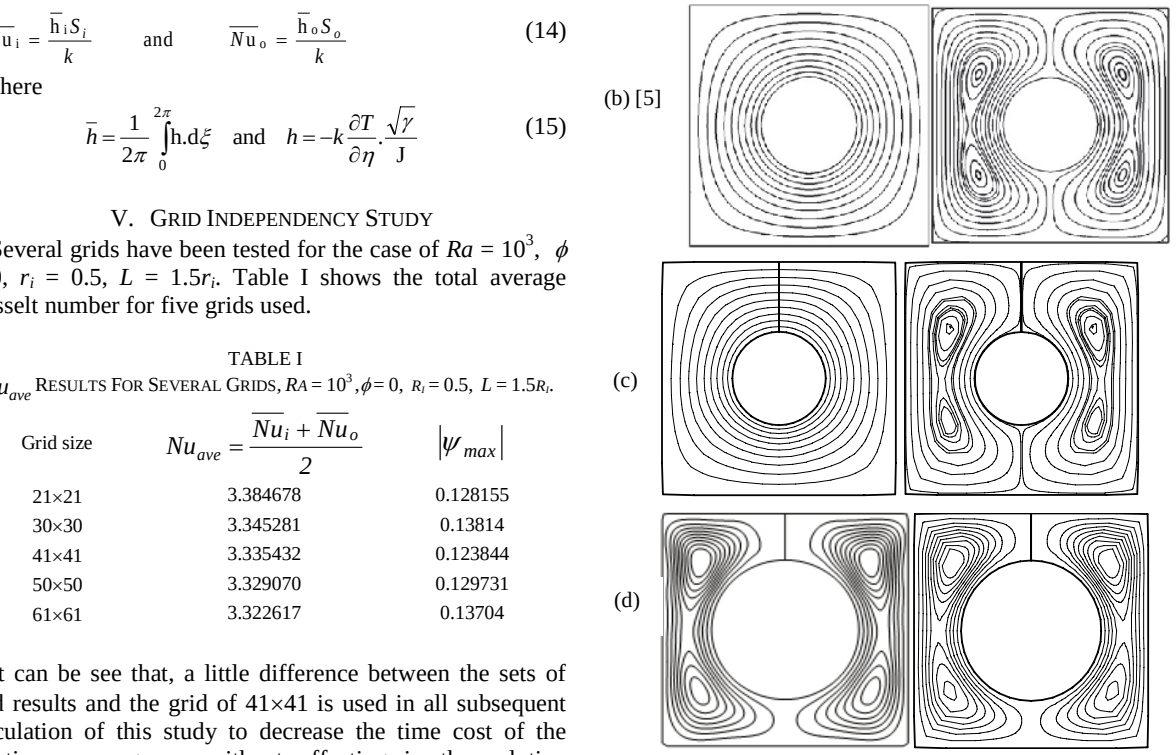

Fig. 3 A comparison of results of references: (a) [2], (b) [5]with (c) present results for (L/D= 0.4), Left side: isotherms & right side: Streamlines, and (d) Streamlines for (L/D =0.2), Left side: Ref.[1] and right side: present results

VII. Results and Discussion

The results are presented for a number of cases (84 different physical domains) corresponding to four different Rayleigh numbers , moreover to seven different inclination angles for the outer square enclosure and three different geometric aspect ratios. The basic features of flow and heat transfer are analyzed with the help of the streamlines pattern and isothermal contours. Also, local Nusselt numbers on the hot and cold isothermal surface of the inner circular cylinder and outer square enclosure are plotted.

A. Flow and Temperature Fields as a Function of AR

The dependence of the flow and thermal fields on *Ar* can be observed in the plots of the streamlines and isotherms for different *Ar* s at different *Ra* shown in Figs 4-5.

For $Ra = 10^3$, the heat transfer in the enclosure is mainly dominated by the conduction mode. The circulation of the flow shows two overall rotating symmetric eddies.

At $Ra = 10^4$, the patterns of the isotherms and streamlines are about the same as those for $Ra = 10^3$. However, a careful observation indicates that the thermal boundary layer on the bottom part of cylinder is thinner than that on the opposite side and the inner lower vortex slightly becomes smaller in size and weaker in strength compared with the upper one, because the effect of convection on heat transfer and flow increases with increasing the Rayleigh number.

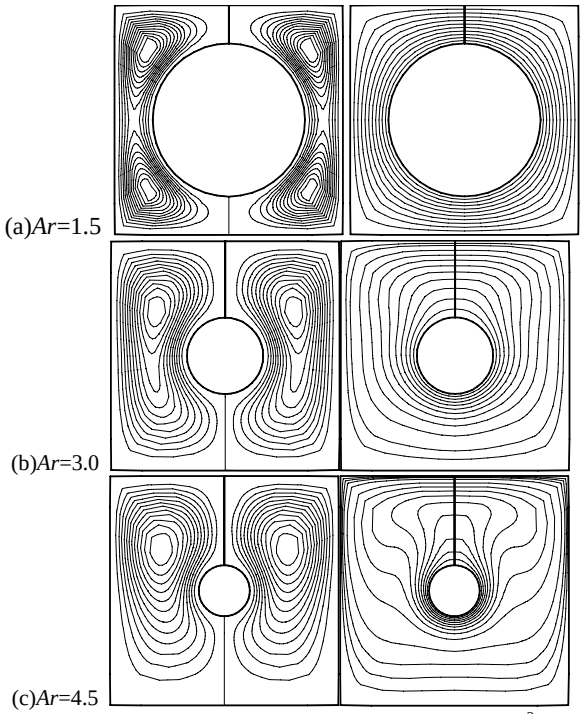

Fig. 4 Streamlines and isotherms for different *Ar* s at $Ra=10^3$ and $\phi = 0$

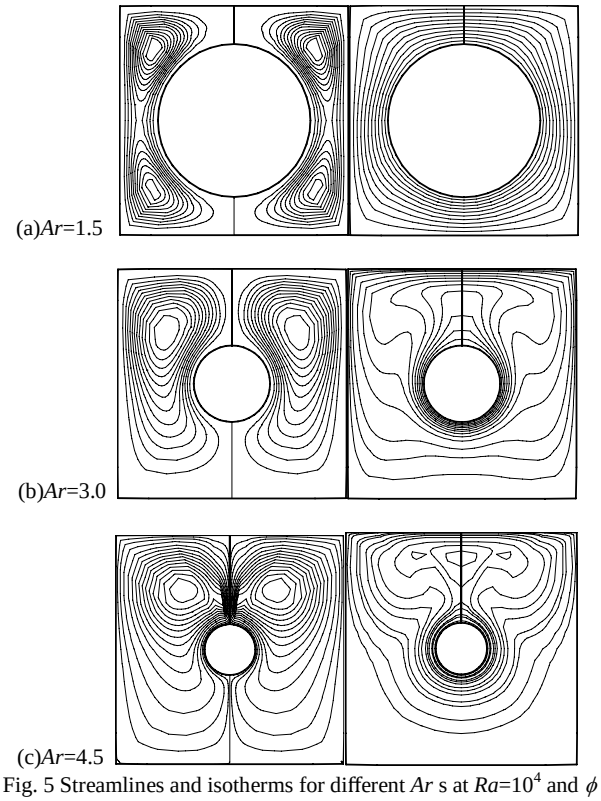

Fig. 5 Streamlines and isotherms for different *Ar* s at $Ra=10^4$ and $\phi = 0$

B.Flow and Temperature Felds as a Function of ϕ

The calculated flow and temperature fields are represented in Figs. 6-8 for angle of inclination variation and different *Ra*.

1. Aspect Ratio = 1.5

Fig. 6 illustrate Streamlines for $Ra=10^5$ at differentϕ. It is observed that the stream lines patterns are almost uniform signifying the relative dominance of diffusion. The size of the vortex formed is large for small angle of inclination and the size reduces for higher angles. With the increase in angle the wall thermal boundary layer thickness increases at the isothermal wall side of the cylinder. As smallerϕ , more number of vortices with complex stream line pattern are evolved. This could be due to the reason that at high *Ra*, the air has higher temperature resulting in large buoyancy forces which leads to the formation and break up of vortices at the corners. As the angle of inclination increases, the number of such regions decrease and a few large vortices can be seen at the left and right walls of the enclosure.

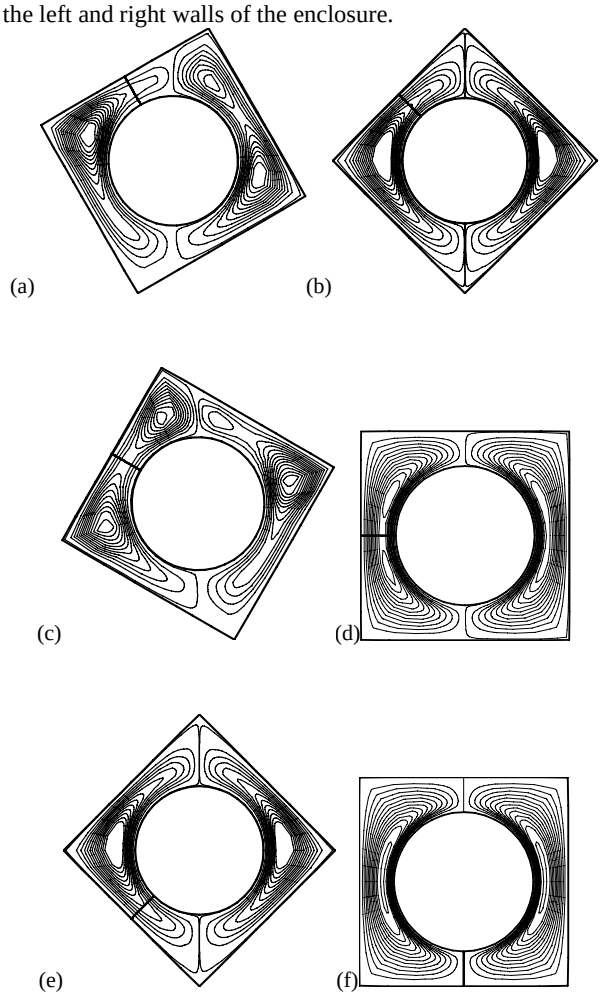

Fig. 6 Streamlines for $Ra=10^5$ at different ϕ (a = -30^o , b = - 45^o , c = -60^o , d = -90^o , e = -135^o and f = -180^o)

2. Aspect Ratio = 3.0

As the angle (ϕ) increases (shown in Fig. 7), the concentration of isotherms at the top corners of the isothermal walls of the enclosure increase showing that significant heat transfer occurs across these corners. Most of the heat transfer on the hot cylinder wall occurs at the bottom. The isotherms are clustered near the circle and heated fluid moves towards to the top corners.

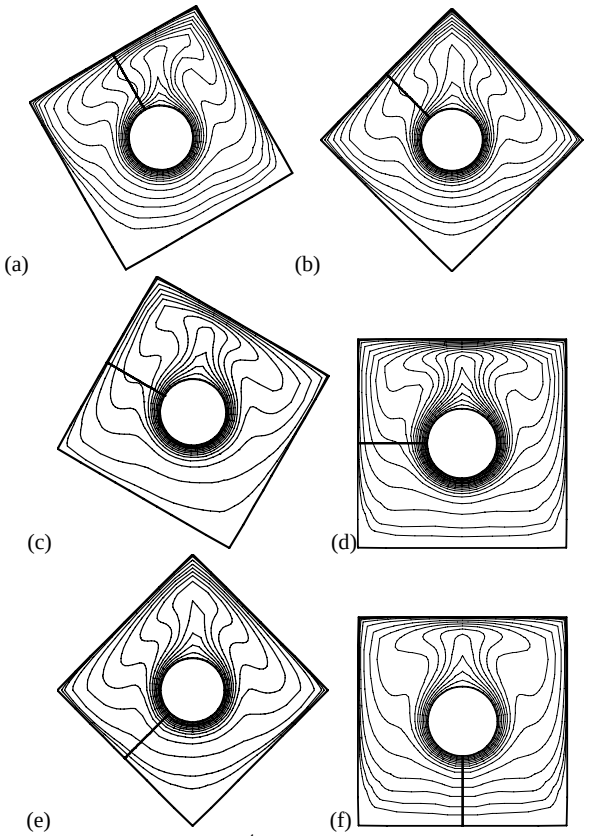

Fig. 7 Isotherms for Ra =10^4 at different ϕ (a = -30^o , b = - 45^o , c = -60^o , d = -90^o , e = -135^o and f = -180^o)

3. Aspect Ratio = 4.5

Fig. 8 Shows velocity components (u,v) contours at different selected ϕ. Fig. 8a and b represent u and v for Ra=10^3 and ϕ=0^o, while Fig. 8c and d represent u and v for Ra=10^4 and ϕ =-45^o. When there is no inclination, the velocity components contours are almost symmetric about the vertical centerline due to the dominance of the conduction. Hence, u_{max}=10.5 and v_{max}=15.7, where the left side counter-clockwise and right side clockwise eddies are separated and located at the center of the enclosure. When ϕ=-45^o, the velocity components contours are not symmetric any more about the vertical centerline, compared to their symmetric shape at ϕ=0^o, where u_{max}=63.3 and v_{max}=55.8. This is due to the inclination and the effect of convection on the flow and heat transfer in the enclosure is increases with increasing Rayleigh number.

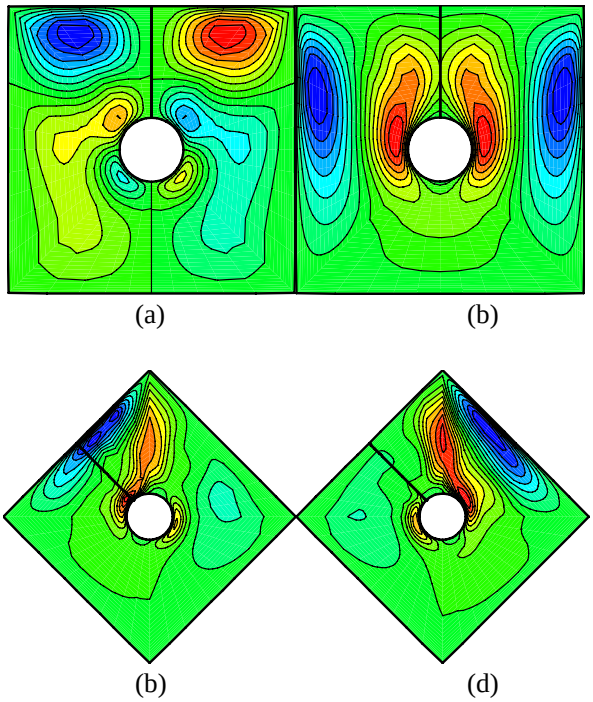

Fig. 8 velocity components contoursat differentϕ. (a&b) represent u and v for Ra =10^3 and ϕ=0^o, (c&d) represent u and v for Ra =10^4 and ϕ=-45^o

C. Average Nusselt Number

The Nusselt numbers is plotted along the isothermal walls for various angle of inclination. Fig. 9a and b shows the distribution of local Nusselt numbers along the hot surface of the inner cylinder and the cold surfaces of the enclosure for different ϕ s at Ra=10^3 and Ar=3.0. The variation of the Nusselt number along the outer enclosure is small, because the distribution of isotherms is almost concentric in the inner cylinder. The distribution of the local Nusselt numbers in the right half of the enclosure are symmetry to the left half about ξ, also to the inner cylinder when ϕ=0^o.

Fig. 10a and b shows the distribution of local Nusselt numbers along the hot surface of the inner cylinder for different ϕ at Ra=10^4 and Ar=1.5 and 3.0. The heat transfer decreases along the cold wall with decreasing diameter of the circular body, or, it increases at hot wall with increasing diameter.

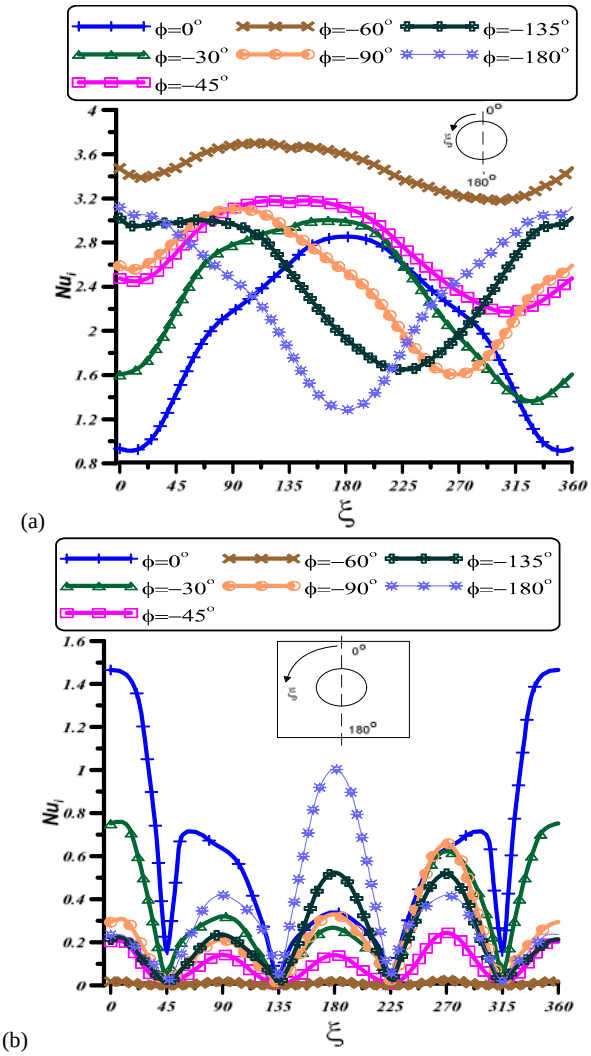

Fig. 9 local Nusselt numbers along: (a) the inner cylinder and (b) the enclosure for different ϕ s at Ra=10^3

Table III lists the average Nusselt numbers for the inner cylinder at different Rayleigh numbers and inclination angles forAr= 4.5. Increase in the angle of inclination results in the increase of Nusselt numbers till around ϕ=-60°, then a small decrease is indicated.

Finally, Fig. 11a and b shows the distribution of local Nusselt numbers along the hot surface of the inner cylinder for different ϕ at Ra=10^5 and 10^6, with Ar= 3.0. The variations of local Nusselt numbers at Ra=10^6 are larger than those at Ra=10^5 due to increasing convection effect with increasing Rayleigh number.

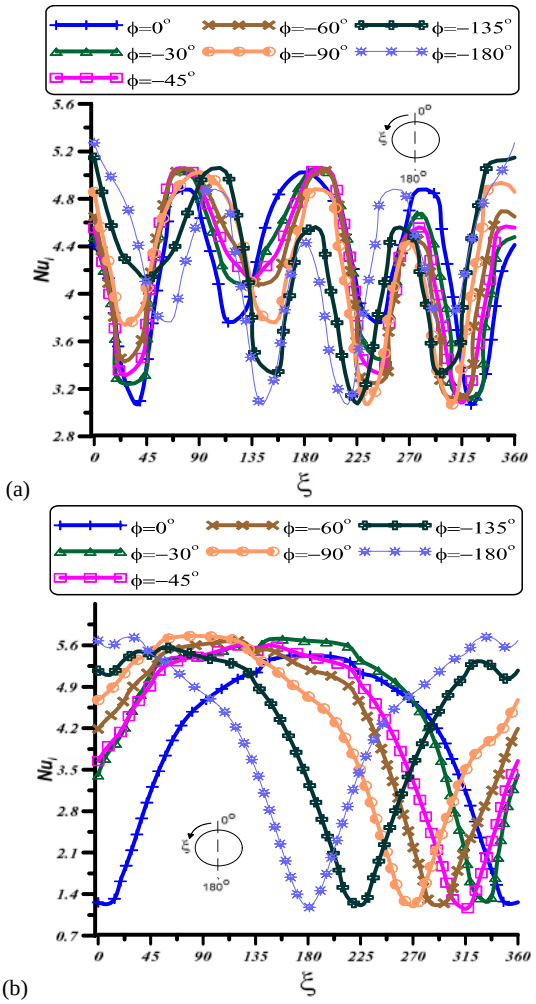

Fig. 10 local Nusselt numbers along the inner cylinder at: Ar= (a)1.5 and (b) 3.0 for different ϕ s at Ra=10^4

TABLE III
AVERAGE NUSSELT NUMBERS AT DIFFERENT RAYLEIGH NUMBERS AND INCLINATION ANGLES FORAr= 4.5

Ra	ϕ	$\overline{Nu_i}$	Ra	ϕ	$\overline{Nu_i}$
	0°	2.44		0°	5.18
	-30°	2.51		-30°	5.12
	-45°	2.59		-45°	4.86
10^3	-60°	3.47	10^4	-60°	4.85
	-90°	2.61		-90°	4.80
	-135°	2.64		-135°	4.80
	-180°	2.66		-180°	4.85
	0°	8.07		0°	13.93
	-30°	8.47		-30°	15.80
	-45°	8.55		-45°	14.71
10^5	-60°	8.14	10^6	-60°	16.05
	-90°	7.91		-90°	16.07
	-135°	8.20		-135°	16.13
	-180°	8.21		-180°	14.37

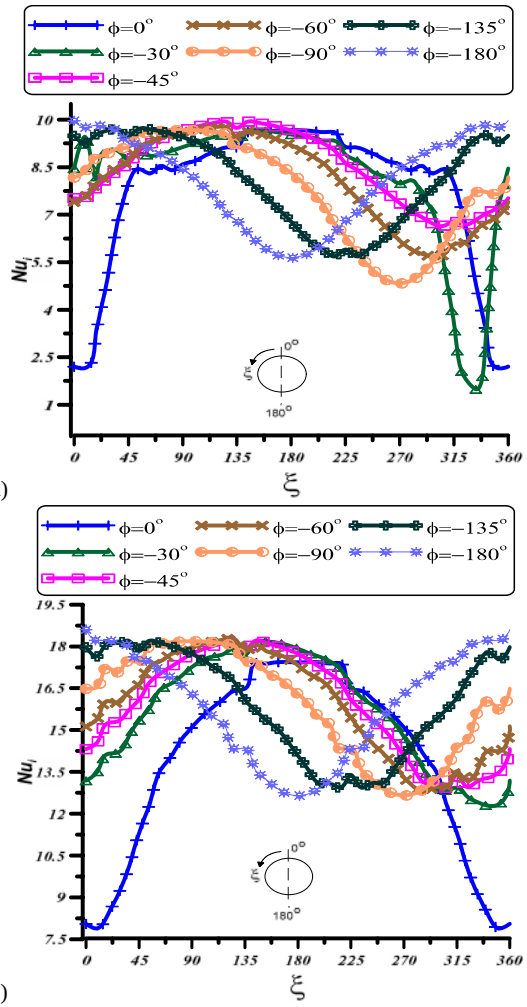

Fig. 11 local Nusselt numbers along the inner cylinder for different ϕs at: Ra= (a) 10^5 and (b) 10^6 and Ar= 3.0

VIII. Conclusions

The present study investigates numerically the characteristics of two-dimensional natural convection problem in the cooled square enclosure with an inner heated circular cylinder. A detailed analysis for the distribution of streamlines, isotherms and Nusselt number carried out to investigate the effect of the aspect ratios for the inner cylinder and the inclination angles for the outer square enclosure on the fluid flow and heat transfer for a range of Rayleigh number. The profiles of Nu_i and Nu_o are not symmetric due to the presence of the secondary vortices and tertiary vortices on the upper surface of the inner cylinder caused by the rising plume from the inner cylinder. The value of Nu_i is larger than that of Nu_o, because the isotherms are formed more densely on the inner cylinder surface than that on the surfaces of the enclosure. At all Rayleigh numbers angle of inclination has nominal effect on heat transfer for different aspect ratios. The influence of inclination angle is particularly strong in the upstream regions on the isothermal walls.

It is observed that the inclination angle can be a control parameter for flow and temperature fields.

Nomenclature

A,B,C,G,H	Transformation parameters
Ar	Aspect ratio
C_P	Specific heat at constant pressure
D	Circle diameter
J	Jacobian
k	Thermal diffusivity of fluid
L	Side length of the square cylinder
T	Dimensionless Temperature
g	Gravitational acceleration
u , v	Dimensionless contravariant velocity components in ξ and η coordinates
x, y	Dimensionless Cartesian coordinates

Greek Symbols

α, γ, σ	Transformation functions
β	Thermal expansion coefficient
ϕ	Inclination angle
ρ_0	Reference viscosity
ξ , η	curvilinear coordinates
ψ	Stream function
ω	Vorticity
ν	Kinematics viscosity

Superscripts

*	Dimensional form

Subscripts

i , o	Inner and outer boundaries (hot and cold surfaces)
max	Maximum value
x, y, ξ, η	Derivative relative to x, y, $\xi$and ηrespectively.

References

[1] Shu, C., and Zhu, Y.D., Efficient computational of natural convection in a concentric annulus between an outer square cylinder and inner circular cylinder, Int. J. Numer. Meth. Fluid 38 (2002) 429-445.

[2] Kim, B.S., Lee, D.S., Ha, M.Y., and Yoon, H.S., A numerical study of natural convection in a square enclosure with a circular cylinder at different vertical locations, Int. J. heat and mass transfer 51 (2008) 1888-1906.

[3] Hyun Sik Yoon, Man Yeong Ha, ByungSoo Kim and Dong Hun Yu, Effect of the position of a circular cylinder in a square enclosure on natural convection at Rayleigh number of 10^7, American Institute of Physics, PHYSICS OF FLUIDS 21 (047101) (2009).

[4] Hakan F. Oztop, Zepu Zhao and BoYu, Fluid flow due to combined convection in lid-driven enclosure having a circular body, International Journal of Heat and Fluid Flow 30 (2009) 886–901.

[5] J.M. Lee, M.Y. Ha and H.S. Yoon, Natural convection in a square enclosure with a circular cylinder at different horizontal and diagonal locations, International Journal of Heat and Mass Transfer 53 (2010) 5905–5919.

[6] Salam Hadi Hussain and Ahmed Kadhim Hussein, Numerical investigation of natural convection phenomena in a uniformly heated circular cylinder immersed in square enclosure filled with air at different vertical locations, International Communications in Heat and Mass Transfer 37 (2010) 1115 –1126.

[7] TalalKassem, Numerical study of the natural convection process in the parabolic–cylindrical solar collector, The Ninth Arab International Conference on Solar Energy (AICSE-9), Kingdom of Bahrain, Desalination 209 (2007) 144–150.

[8] C. Shu ,Q.Yao , K. S. Yao and Y. D. Zhu , Numerical analysis of flow and thermal fields ia arbitrary eccentric annulus by differential quadrature method, Heat and Mass Transfer 38 (2002) 597-608.
[9] Arnab Kumar De and AmareshDalal , A numerical study of natural convection around a square horizontal heated cylinder placed in an enclosure, International Journal of heat mass transfer 49 (2006) 4608-4623.
[10] WenRuey Chen, Natural convection heat transfer between inner sphere and outer vertically eccentric cylinder, International Journal of Heat and Mass Transfer 53 (2010) 5147–5155.
[11] XuXu, Gonggang Sun, Zitao Yu, Yacai Hu, Liwu Fan, Kefa Cen, Numerical investigation of laminar natural convective heat transfer from a horizontal triangular cylinder to its concentric cylindrical enclosure, International Journal of Heat and Mass Transfer 52 (2009) 3176–3186.
[12] Zi-Tao Yu, Li-Wu Fan, Ya-Cai Hu and Ke-Fa Cen, Prandtl number dependence of laminar natural convection heat transfer in a horizontal cylindrical enclosure with an inner coaxial triangular cylinder, International Journal of Heat and Mass Transfer 53 (2010) 1333–1340.
[13] Manab Kumar Das and K . Saran Kumar Reddy, Conjugate natural convection heat transfer in an inclined square cavity containing a conducting block, International Journal of Heat and Mass Transfer 49 (2006) 4987–5000.
[14] YasinVarol, Hakan F. Oztop, AhmetKoca and FilizOzgen, Natural convection and fluid flow in inclined enclosure with a corner heater, Applied Thermal Engineering 29 (2009) 340–350.
[15] H.F. Nouanegue, A. Muftuoglu, E. Bilgen, Heat transfer by natural convection, conduction and radiation in an inclined square enclosure bounded with a solid wall, International Journal of Thermal Sciences 48 (2009) 871–880.
[16] F.A. Munir, N.A.C. Sidik and N.I.N. Ibrahim, Numerical Simulation of Natural Convection in an Inclined Square Cavity, Journal of Applied Sciences 11 (2) (2011) 373-378.